2011

The behavior of nanothermite reaction based on Bi2O3/Al

L. Wang
University of Houston

D. Luss
University of Houston

Karen S. Martirosyan
The University of Texas Rio Grande Valley

The behavior of nanothermite reaction based on Bi_2O_3/Al

L. Wang,[1] D. Luss,[1] and K. S. Martirosyan[2,a)]
[1]*Department of Chemical and Biomolecular Engineering, University of Houston, Houston, Texas 77204, USA*
[2]*Department of Physics and Astronomy, University of Texas at Brownsville, 80 Fort Brown, Brownsville, Texas 78520, USA*

(Received 1 July 2011; accepted 1 September 2011; published online 13 October 2011)

We studied the impact of aluminum particle size and the thickness of surrounding alumina layer on the dynamic pressure discharge of nanothermite reactions in the Bi_2O_3/Al system. A pressure discharge from 9 to 13 MPa was generated using as-synthesized Bi_2O_3 nano-particles produced by combustion synthesis and Al nanoparticles with size from 3 μm to 100 nm. The maximum reaction temperature was measured to be ~2700 °C. The estimated activation energy of the reaction was 45 kJ/mol. A very large (several orders of magnitude) difference existed between the rate of the pressure pulse release by nanothermite reactions and by thermite reactions with large aluminum particles. The maximum observed pressurization rate was 3200 GPa/s. The time needed to reach the peak pressure was 0.01 ms and 100 ms for aluminum particles with diameter of 100 nm and 70 microns, respectively. The discharge pressure was a monotonic decreasing function of the thickness of the surrounding alumina layer. © *2011 American Institute of Physics*. [doi:10.1063/1.3650262]

I. INTRODUCTION

Thermite is pyrotechnic mixtures of metal powders (fuel, Al, Mg, etc.) and metal oxides (oxidizer, Fe_2O_3, WO_3, MoO_3, etc.) that can generate an exothermic oxidation-reduction reaction referred to as a thermite reaction. A thermite reaction releases a large amount of energy and can generate rapidly extremely high temperatures. The intimate contact between the fuel and oxidizer can be enhanced by use of nano instead of micro particles.[1,2] This decreases the mass transport limitations and increases the reaction rate and reactivity of the thermite mixture. Nanoenergetic materials (NM) also known as metastable intermolecular composites (MIC) have various potential applications as propellants, explosives, and primers. They can have higher energy densities than conventional explosives[3,4] and can generate shock wave with velocities of up to 2500 m/s.[5–7] Their application is currently the subject of extensive research.[8–11] Thermodynamic calculations of the adiabatic temperature, equilibrium composition, and reaction enthalpy help select an MIC mixture from a large number of candidate thermite mixtures. The calculations predict that the volumetric energy release by several thermite reactions exceeds that of commercial explosives and propellants.[12]

Extensive research has been conducted in this area. Pantoya *et al.*[4] studied the dependence of the ignition and flame propagation features during the MoO_3/Al nanothermite reaction. Sun *et al.*[10] reported that the reactivity of mixtures containing aluminum nano-particles significantly exceeded those containing micron size particles. The reactivity of the thermite mixture is strongly depended on the particle size distribution. While great progress has been made in the enhancing of the energy release and shock wave velocity of nanothermite materials, the reaction mechanism still is not fully understood. Most research focused on the impact of the reactant particle size on the ignition temperature and combustion front velocity.[10,13–15] Until recently, very few reports have considered gas evolution during nanothermite reactions.[5,6,11,16]

Recently, we have shown that the Bi_2O_3/Al thermite reaction generates the highest pressure pulse among numerous thermite reactions.[17] Using a 0.5 g mixture of crystalline Bi_2O_3 nano-particles, synthesized by a modified solution combustion method,[18] and Al the nanothermite mixture generated a peak pressure of 12 MPa in a closed vessel ($V = 0.342$ L). The corresponding maximum pressure × volume per mass (PV/m) value was 8.6 kPa · m^3/g. We report here a study of the dependence of the pressure discharge during Bi_2O_3/Al nanothermite reaction on the aluminum particle size (100 nm, 3 μm, 20 μm, and 70 μm) and the impact of the thickness of the alumina layer surrounding the aluminum particles.

II. EXPERIMENTAL SYSTEMS AND PROCEDURES

Bismuth trioxide nanoparticles were prepared by a modified aqua combustion synthesis from bismuth nitrate and glycine (details reported in Ref. 17). The reaction mixtures contained the as-synthesized Bi_2O_3 nano-particles and aluminum powders with an average particle size of 100 nm, 3 μm, 20 μm, 70 μm purchased from Sigma-Aldrich. The aluminum powders were stored under nitrogen (99.9 vol. % N_2 with 50 ppm O_2) in a glovebox to prevent oxidation and contamination by impurities present in the air. Most nanothermite reactions are highly exothermic and the mixtures may spontaneously detonate in some cases due to heating, friction, and/or electrostatic discharge built up when the precursors are mixed or ground together. The mixtures were mixed in hexane to prevent electrostatic charge buildup that may cause ignition or explosion of the powders during the mixing and handling. Stoichiometric mixtures of the reactants (bismuth oxide 80 wt % and Al particles 20 wt %) were mixed in a closed cylindrical container (volume 68 cm^3) containing hexane and nitrogen for different mixing time (up to 30 h) by

a)Author to whom correspondence should be addressed. Electronic mail: karen.martirosyan@utb.edu.

a rotary mixing machine (rotary speed 240 rpm). The weight ratio of the sample to the mixing balls was 3 g/70 g.

The pressure release was measured in a commercial stainless steel, high pressure, cylindrical reactor, 30.7 mm inner diameter, and 115 mm long (Parr, model 1108, V = 0.342 L) A pressure up to 14 MPa was measured by a high-frequency pressure transducer (PCB Piezotronics Inc.) on top of the reactor. A schematic of the system is shown in Fig. 1(a). A loose reactant mixture (0.1–0.5 g) was placed in a ceramic boat in the center of the reactor. Due to the safety consideration, the sample mass did not exceed of 0.5 g. The reactant mixture was ignited by an electrically heated coil inserted into the bottom of the sample. The pressure signal was recorded and processed by an Omega data acquisition board connected to a PC with a resolution of 1 μs.

The particles size and surface morphology of the samples were determined by high-resolution transmission electron microscope (HRTEM, JEOL JEM-2000 CX2) and scanning electron microscope (SEM, JEP JSM-6400). The sample surface radiation (temperature) was measured and recorded in an open stainless steel cylindrical reactor (38 mm ID and 12 mm long) by a high frequency infrared (IR) camera (FLIR, SC4000). A gold plated mirror was positioned on the top of the reactor inclined by 45° to reflect the temperature radiation to the IR camera. The reactant mixture was loosely placed inside an alumina ring (10 mm ID and 5 mm high) on the bottom of the reactor and ignited by an electrically heated coil. The recorded images determined the maximum temperature and shape of the thermal front propagation.

The velocity of the propagating reaction front was determined from the distance between the two photo-detectors and the difference in the arrival time of the temperature front. A schematic of this experimental set-up is shown in Fig. 1(c). A hollow space existed in the stainless steel reactor (diameter 2 mm, height 40 mm). Two tiny photodiodes were placed into two holes (Ø = 1 mm) in the reactor with a distance of 20 mm between them. To measure the reaction front velocity we loaded into the hollow space (~0.1 g) of the Bi_2O_3/Al mixture and ignited the reaction by a thin electrical coil inserted into one side of the reactant. The propagating thermal front emitted high intensity light, that the photodiodes transformed into transient electrical signals. The photodiodes signals were recorded by a data acquisition board connected to a PC with a time resolution of 1 μs.

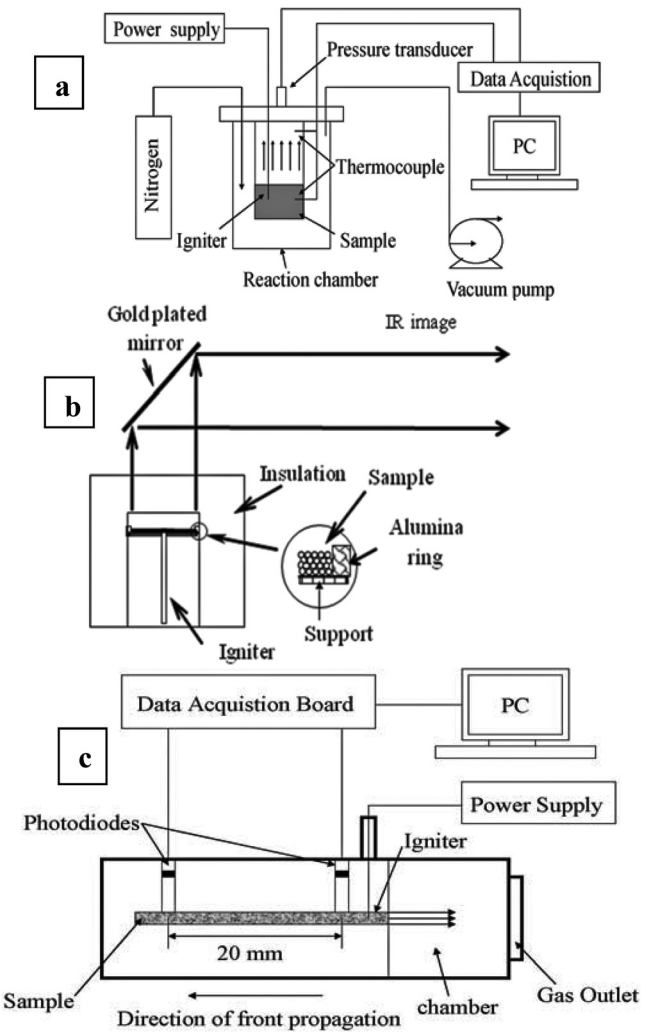

FIG. 1. Schematic of experimental systems for measuring and recording of (a) – pressure evolution, (b) – spatial-temporal temperature, and (c) – thermal front velocity.

III. EXPERIMENTAL RESULTS

A TEM of the mixed Bi_2O_3/Al (100 nm) nanothermite mixture (Fig. 2) showed that the bismuth trioxide nanoparticles were well distributed among the aluminum particles. The average diameter of the crystalline Bi_2O_3 nanoparticles was about 40–50 nm. The diameter of the aluminum particles surrounded by a thin aluminum oxide layer was in the range of 50–150 nm. SEM micrographs of aluminum micro powders with average particle size of 3 and 20 μm before and after mixing with bismuth trioxide (Fig. 3), confirmed that the mixing did not change the shape and size of the 3 μm aluminum particles. Again, the Bi_2O_3 nano particles were spread among the spherical aluminum particles.

IR thermal images revealed that the temperature during the Bi_2O_3/Al (100 nm) reaction rose at least to 2700 °C. This

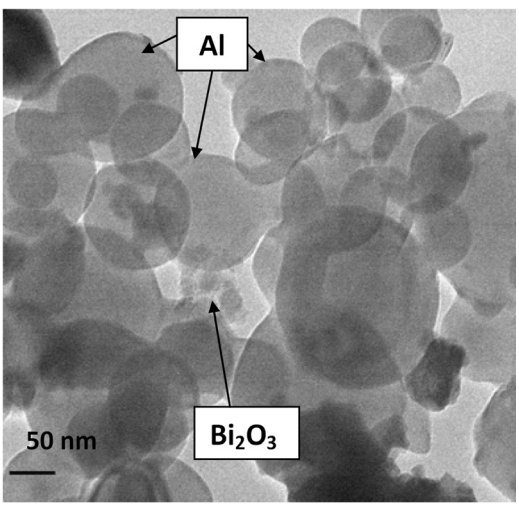

FIG. 2. TEM image of a mixture of 100 nm aluminum and bismuth trioxides particles.

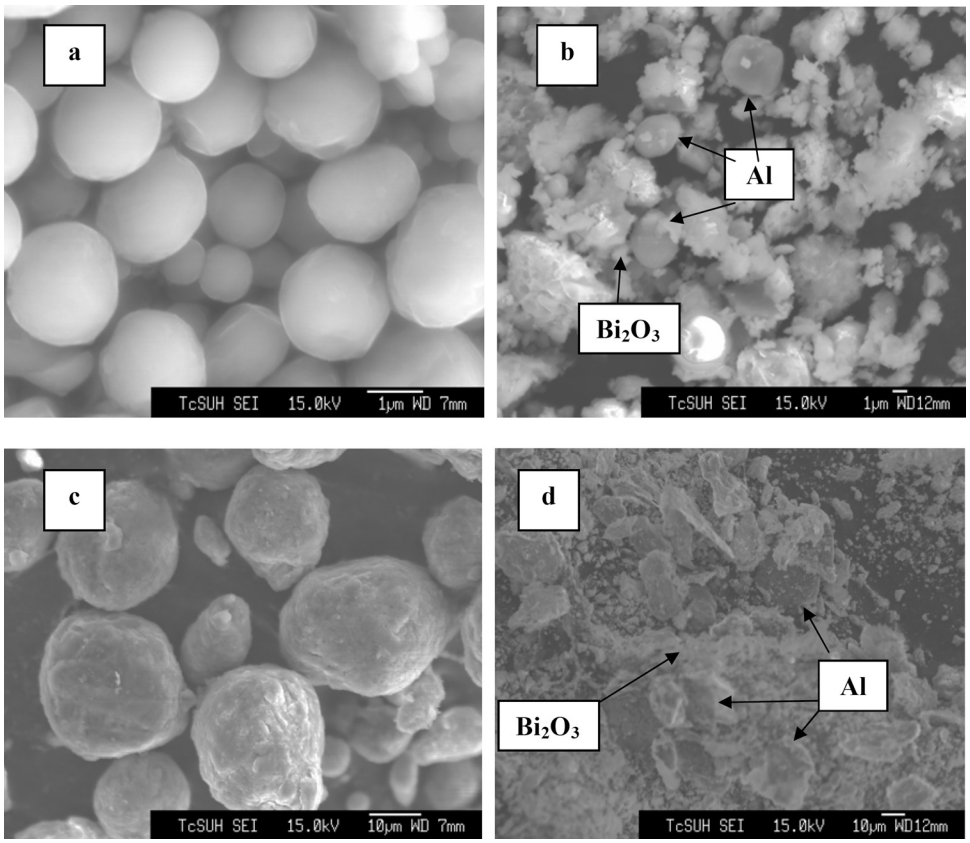

FIG. 3. SEM images of (a) 3 μm aluminum; (b) Bi_2O_3/aluminum (3 μm); (c) 20 μm aluminum; and (d) Bi_2O_3/aluminum (20 μm).

high temperature caused evaporation of Bi, the boiling temperature of which is 1564 °C. This measured temperature is consistent with thermodynamic analysis that estimates the adiabatic temperature to be 2980 °C. Figure 4 shows spatial temperature distribution during the thermite reaction of Bi_2O_3/Al with an aluminum particle with an initial average size of 20 μm. It shows that the maximum temperature of the Al micro particles was about 1700 °C, which was sufficiently high to vaporize the Bi product. Heat loss during the slow reaction of the large particles is probably the cause for lowering the maximum temperature from the adiabatic temperature.

The impact of the Bi_2O_3/Al (100 nm) sample mass (0.1–0.5 g) on the pressure release is shown in Fig. 5. The pressure measurements were repeated three times for each nanothermite sample. The pressure of the nano particle mixture was reproducible within the range of 10%. The peak pressure in all these experiments was reached in about 0.1 ms. It was proportional to the weight of the sample. This data suggest that a simple relation exists between the peak pressure (P) and the weight of the Bi_2O_3/Al sample (m), i.e., $P = 22.85\,m$, where m is the sample weight (g). This relation is shown as an inset in Fig. 5.

The mixing of the nanothermite mixture is very important for getting homogeneous particle distribution, avoiding agglomerates and electrostatic discharge. The quality of the mixing affects the reaction behavior. We studied the impact of the mixing time of the Bi_2O_3/Al mixtures on the velocity

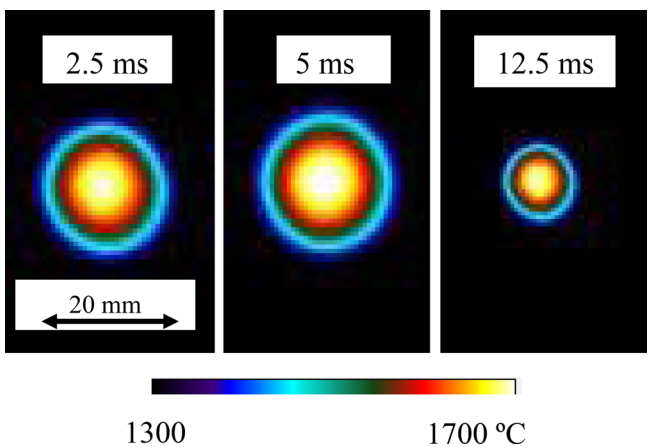

FIG. 4. (Color online) IR thermal images during reaction of Bi_2O_3/Al, aluminum particles size 20 μm.

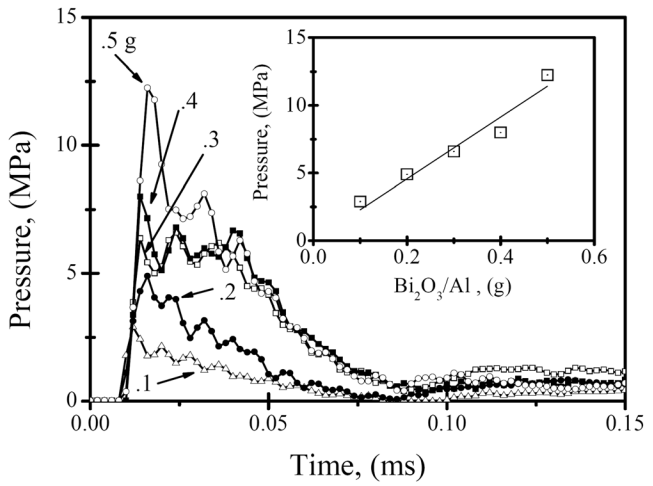

FIG. 5. Dependence of temporal pressure evolution on sample weight (0.1–0.5 g) during Bi_2O_3/Al (100 nm) nanothermite reaction.

of the reaction front (Fig. 6(a)). A maximum front velocity of 2500 m/s was obtained for a sample following 6 h of mixing. A much lower front velocity of ~760 m/s was obtained using a mixture that was mixed for only 0.5 h. This suggests that the thermite mixture was not well mixed and homogeneous after 0.5 h of mixing. The front velocity decreased to 1030 m/s, following 30 h of mixing. The SEM image of this mixture shown in Fig. 6(b) revealed that this was due to mixture agglomeration. Several agglomerated clusters in the range of 1–10 μm were clearly visible.

The kinetics of the Bi_2O_3/Al (100 nm) nanothermite reaction was studied by thermal analysis under different heating rates. The reaction kinetics and ignition characteristics were determined by the differential scanning calorimetry approach. Figure 7(a) shows that the ignition temperature increased from 476 °C to 524 °C as the heating rate increased from 53.4 °C/min to 92.4 °C/min. The apparent activation energy E_a (kJ/mol), which is defined as the minimum energy needed to initiate the reaction, was calculated by the Starink relation:[19]

$$\ln\left\{\frac{T^{1.8}}{\beta}\right\} = (1.0070 - 1.2 \times 10^{-5} E_a)\frac{E_a}{RT} + \text{const},$$

where β is the heating rate (K/min), T the peak temperature of exothermic curve (K), and R the universal gas constant. It follows that E_a can be estimated from the slope of the linear graph of $\ln(T^{1.8}/\beta)$ versus 1/T. The iso-conversion Starink method was used to estimate the activation energy, as shown by Fig. 7(b). It was estimated to be 45 kJ/mol.

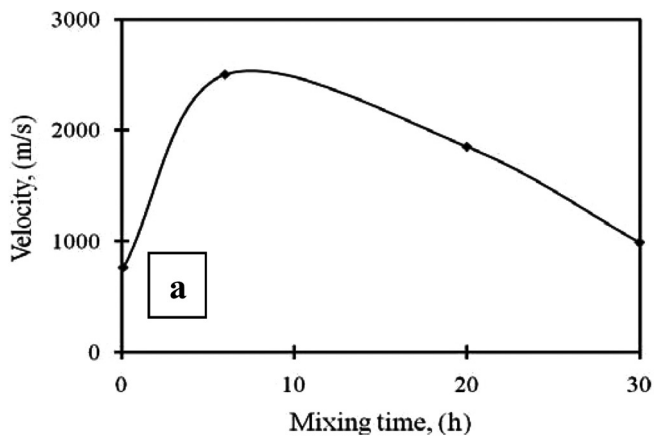

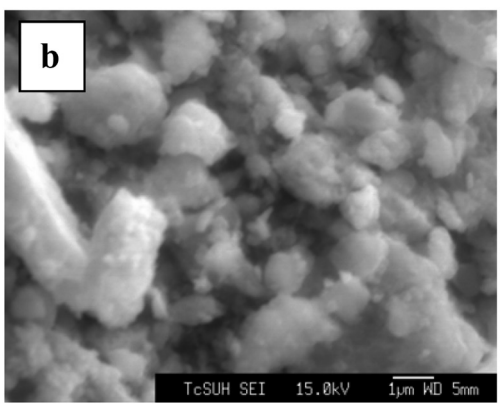

FIG. 6. (a) - Dependence of thermal front velocity on the mixing time during Bi_2O_3/Al nanothermite reaction; (b) - the SEM image of the nanothermite mixture after 30 h mixing.

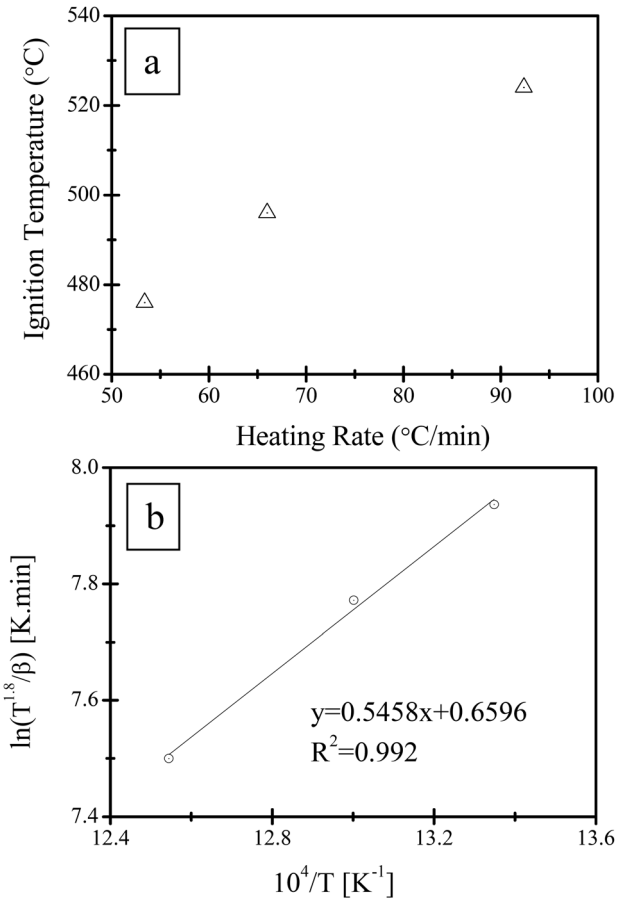

FIG. 7. (a) - Ignition temperature of Bi_2O_3/Al (100 nm) nanothermite reactions at different heating rates and (b) - Arrhenius plot for the exothermic peaks of the DSC curves.

The aluminum particle size has a strong impact on the thermal front velocity and the gas discharge. The experiments reported in Fig. 8 show that as the aluminum particle size decreased from 70 microns to 100 nm the thermal front velocity increased from 90 to 2500 m/s and the peak pressure from 0.7 to 12.6 MPa. These experiments demonstrated that

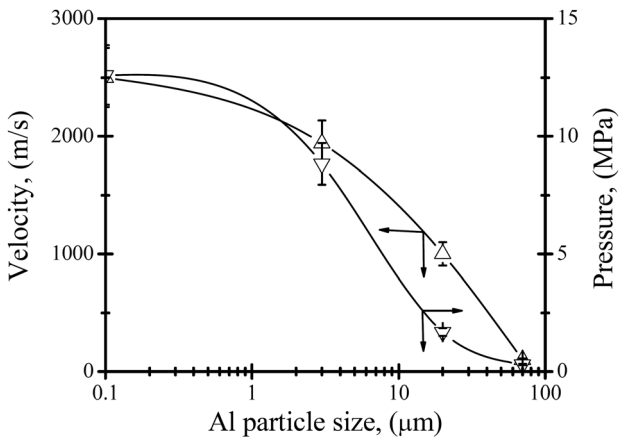

FIG. 8. Dependence of peak pressure and thermal front velocity on the aluminum particle size during Bi_2O_3/Al nanothermite reactions.

the Al powder particle size significantly affected the pressure release and front propagation behavior.

Figure 9 describes the impact of the aluminum particle size on the pressure rise during the Bi_2O_3/Al reactions. Figure 9(a) shows that a pressure peak of 12.6 and 8.82 MPa was generated by the Bi_2O_3/Al reaction, using Al particles with a diameter of 100 nm and 3 μm, respectively. Both reaction mixtures generated a similar dynamic pressure release and the reaction duration in both were about 0.1 ms. However, the time needed to reach the peak pressure for nanoparticles were ~0.01 ms, half of that for 3 μm particles. Figure 9(b) shows the pressure rise using Al particles with diameters of 20 and 70 μm. These reactions lasted for a much longer time (0.6 and 400 ms for a mixture with Al particles diameter of 20 and 70 μm, respectively). The peak pressure decreased from 1.68 to 0.7 MPa as the Al diameter increased.

To study the behavior of the pressure discharge (Fig. 10), we conducted Bi_2O_3/Al (100 nm) nanothermite reaction under different environments (air, nitrogen, and vacuum). The pressure generated during the reaction in the atmospheric air is lower than that in either the vacuum or the nitrogen environment. This is most probably because the oxygen in the air oxidized some nano-aluminum particles, decreasing the effective Al content and lowering the overall released energy and reaction rate. The fact that the peak pressure under the atmospheric pressure of nitrogen and vacuum environment are similar suggests that the fast evaporation of the Bi produces the pressure rise during the reaction.

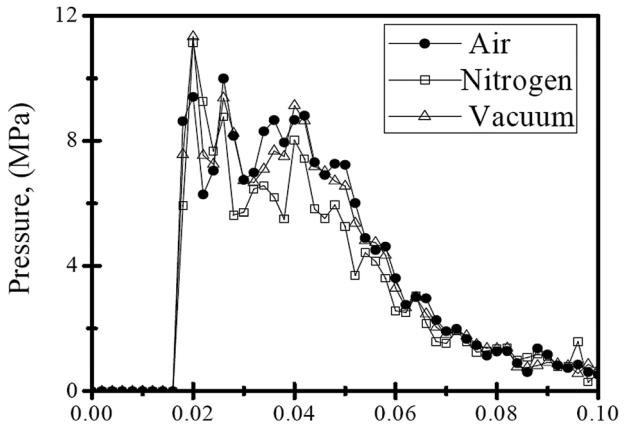

FIG. 10. Temporal pressure rise during Bi_2O_3/Al nanothermite reactions under different environments (air, nitrogen, and vacuum).

The aluminum particles are usually surrounded by a thin layer of alumina (aluminum oxide). The thickness of this layer affects the mechanism and dynamics of the nanothermite reaction. Thus, we used a TEM imaging (Fig. 11) to study the impact of exposure in air (0 to 90 min) of the fresh Bi_2O_3/Al (100 nm) mixture. As Fig. 12 shows the layer thickness was about 1 nm before exposure in air and reached

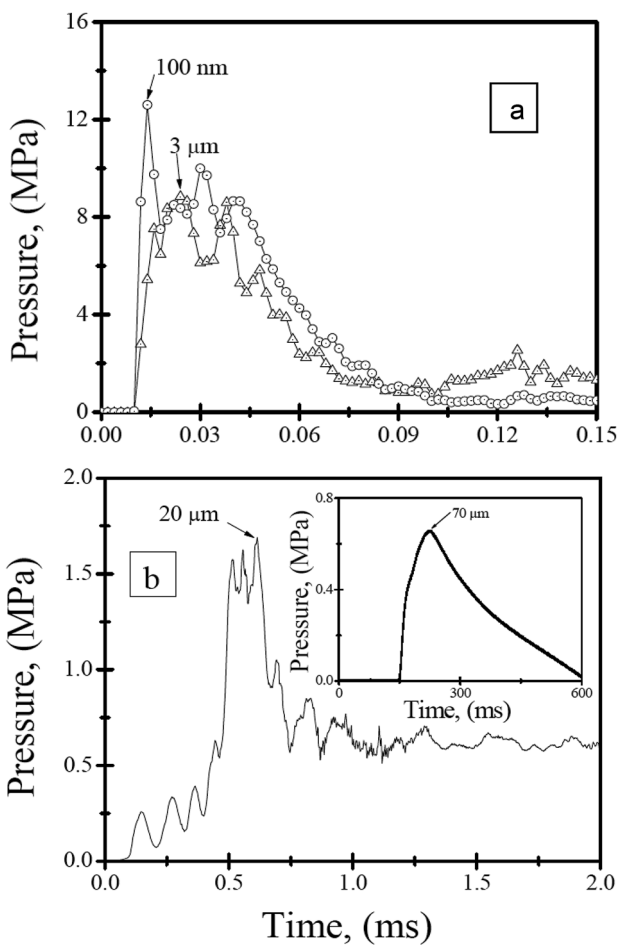

FIG. 9. Influence of aluminum particle size on temporal pressure rise during Bi_2O_3/Al nanothermite reactions (a) - aluminum 100 nm and 3 μm; (b) - aluminum 20 μm and 70 μm (inset).

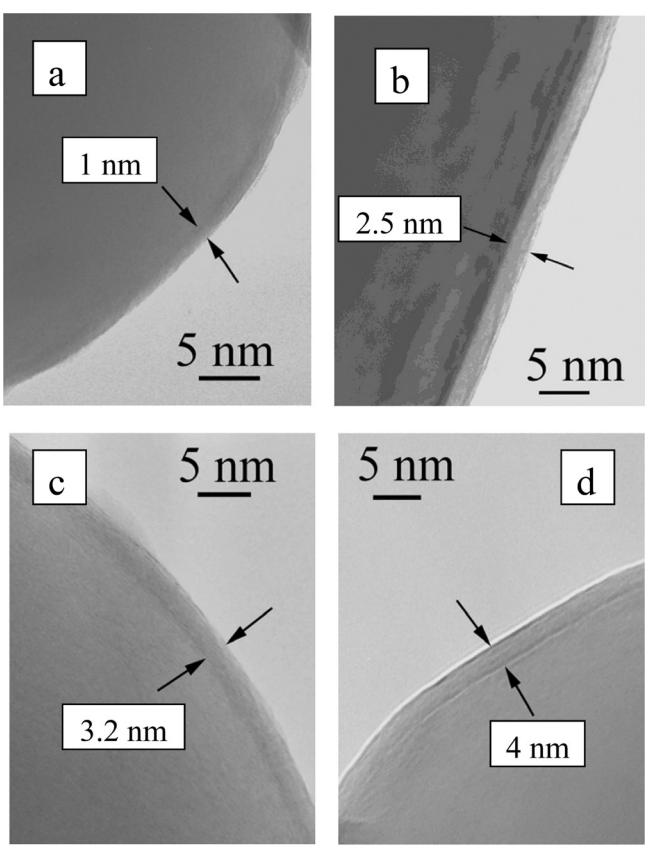

FIG. 11. TEM images of Al nanoparticles oxide layer following different exposure time in air: (a) 0 min; (b) 5 min; (c) 20 min; and (d) 90 min.

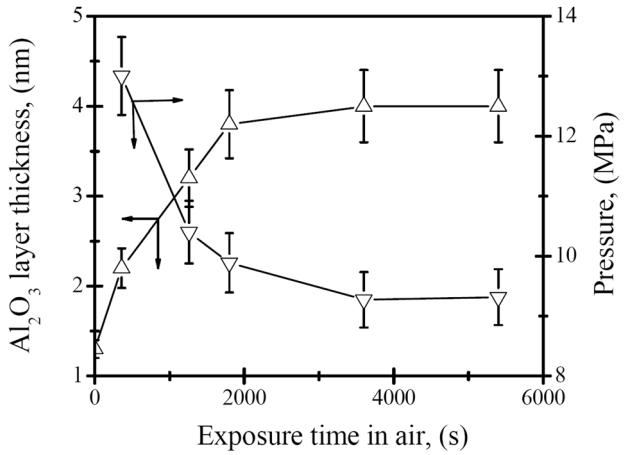

FIG. 12. Dependence of alumina layer thickness and peak pressure on the exposure time in air during Bi_2O_3/Al nanothermite reactions. (m = 0.5 g, V = 0.342 L).

after 30 min an asymptotic value of about 4 nm. It did not grow further following additional exposure. The dependence of the alumina layer thickness and peak pressure release on the aluminum particles exposed time in air is shown in Fig. 12. As the alumina layer increased from 1 nm to 4 nm the peak pressure decreased from 13 to 9.3 MPa. Each of these experiments was conducted with a sample size of 0.5 g.

IV. DISCUSSIONS AND CONCLUDING REMARKS

Following a short exposure to air, aluminum nanoparticles are surrounded by an oxide shell 1–3 nm thick. This passivation layer protects the solid aluminum core from oxidation and has a critical impact on the behavioral features of the thermite reactions.[20–24] Two main thermite reaction mechanisms have been proposed: A melt-dispersion mechanism[25,26] and a diffusion-controlled heterogeneous oxidation mechanism.[27–29] The *melt dispersion* mechanism claims that external heating melts the aluminum inside the exterior alumina layer. The corresponding volume expansion generates a large pressure gradient (up to 88 000 atm), cracking the alumina shell and ejecting small molten Al clusters outwards, initiating a rapid exothermic reaction between the aluminum and the oxidizer. This fast reaction leads in some cases to an explosion.[25,26]

Melting of the aluminum increases its rate of diffusion through the alumina layer. The *diffusion-controlled heterogeneous oxidation model* claims that the ignition is caused by aluminum that diffuses through the oxide shell. An electric field forms that increases the rate of the Al^{3+} and O^{2-} ions diffusion through the shell.[30,31] The outward flux of aluminum then reacts with the oxidizer.[10] Henz[32] and Nakamura[33] investigated the impact of the electric field during nanothermite reaction by molecular dynamic simulations and experiments. They applied a modified Mott Cabrera model to predict the accelerated diffusion of Al^{3+} and O^{2-} ions. The main difference between the two mechanisms is how the molten aluminum liquid gets out of the alumina layer and reacts with the oxidizer, and how long it takes to complete this process. At present there exists no conclusive resolution of which of the two different mechanisms is the correct one. Neither model can predict the time at which the released pressure pulse will reach its maximum and its dependence on the particle size and surrounding shell nor that of complete consumption of the aluminum. More experiments and modeling are needed to provide that information.

The experiments revealed a very large (several orders of magnitude) dependence of the rate of the pressure pulse release on the Al particle size in the mixture. (For example, the time needed to reach the peak pressure was 0.01 ms and 100 ms for aluminum particles of diameter of 100 nm and 70 microns, respectively). The difference may be due to two effects, the more rapid heating and melting of aluminum in small particles and the impact of particle size on the melting temperature. The rate of particle heating by conduction is inversely proportional to the square of the particle radius. When the external temperature reaches the aluminum melting temperature, all the aluminum inside nano-particles rapidly melts. Due to the difference in the particle diameter, the melting inside large aluminum particles is much slower. Thus, only a small fraction of the solid aluminum in the large particles melts during the time that the melting was complete in the nano-particles. After the molten, aluminum liquid either spilled out of the alumina shell or diffused through the alumina layer and contacted the Bi_2O_3, the exothermic thermite reaction ignites, releasing rapidly a large amount of heat and gas. For large aluminum particles, the reaction between the molten Al and Bi_2O_3 started while some of the aluminum is still a solid and it takes some time to melt it.

A second effect is the decrease in the melting temperature of nano-particles. The aluminum in nano particles may exhibit a melting temperature depression following the Gibbs-Thomson relationship based on surface tension effects.[34,35] It was reported that the ignition temperature of nano-aluminum particles (300–600 °C) is lower than the common aluminum melting temperature of 660 °C.[36,37] On the other hand, it was reported that the external alumina layer increases the ignition temperature of large aluminum particles well above the aluminum melting temperature from 660 to 1500 °C due to the different thickness and polymorphic phase transitions of the surrounding alumina layer (amorphous Al_2O_3, γ-Al_2O_3, θ-Al_2O_3 and α-Al_2O_3).[37,38] For example, the ignition temperature of 15–70 μm aluminum particles was reported to be in the range of 1640–2000 °C, close to the melting temperature of alumina (2050 °C).[39,40] The higher melting temperature and longer melting time of the aluminum in large particles increases the duration of the time needed for the liquid aluminum to contact and react with the oxidizer. This explains why nano-particles lead to much more rapid pressure release than micron size particles.

The thinner the alumina layer is, the easier it is for the molten alumina to be released through the alumina layer and ignite the reaction. The peak pressure generated by the nanothermite reactions is proportional to the reactants reactivity. The experimental results reported in Fig. 12 indicate that any accidental short exposure of either the aluminum particles or of the reaction mixture to air is not expected to have a large effect on the peak pressure.

ACKNOWLEDGMENTS

The research was sponsored by the Air Force Research Laboratory under agreement number FA8650-07-2-5061, NSF grant number 0933140 and by the BSF. The U.S. Government is authorized to reproduce and distribute reprints for Governmental purposes not withstanding any copyright notation thereon. The views and conclusions contained herein are those of the authors and should not be interpreted as necessarily representing the official policies or endorsements, either expressed or implied, of Air Force Research Laboratory or the U.S. Government. We also would like to thank Dr. Rusakova for assistance in TEM imaging.

[1]E. L. Dreizin, Prog. Energ. Combust. **35**, 141 (2009).
[2]D. Dlott, Mater. Sci. Technol. **22**, 463 (2006).
[3]C. Rossi, K. Zhang, D. Esteve, P. Alphonse, P. Tailhades, and C.Vahlas, J. Microelectromech. S. **16**, 919 (2007).
[4]M. L. Pantoya and J. J. Granier, Propellants, Explos. Pyrotech. **30**, 53 (2005).
[5]K. S. Martirosyan, L. Wang, and D. Luss, Chem. Phys. Lett. **483**, 107 (2009).
[6]K. S. Martirosyan, L. Wang, A. Vicent, and D. Luss, Propellants, Explos. Pyrotech. **34**, 532 (2009).
[7]K. S. Martirosyan, J. Mater. Chem. **21**, 9400 (2011).
[8]S. F. Son, B. W. Asay, T. J. Foley, R. A. Yetter, M. H. Wu. and G. A. Risha, J. Propul. Power. **23**, 715 (2007).
[9]K. Sullivan, G. Young, and M. R. Zachariah, Combust. Flame. **156**, 302 (2009).
[10]J. Sun, M. Pantoya, and S. Simon, Thermochim. Acta. **444**, 117 (2006).
[11]J. A. Puszynski, C. Bulian, and J. Swiatkiewicz, J. Propul. Power. **23**, 698 (2007).
[12]S. H. Fisher and M. C. Grubelich, in Proceedings of 24th International Pyrotechnics Seminar (USA, 1998), pp. 231–286.
[13]G. M. Dutro, R. A. Yetter, G. A. Risha, and S. F. Son, P. Combust. Inst. **32**, 1921 (2009).
[14]R. Shende, S. Subramanian, S. Hasan, S. Apperson, R. Thiruvengadathan, K. Gangopadhyay, S. Gangopadhyay, P. Redner, D. Kapoor, S. Nicolich, and W. Balas, Propellants, Explos. Pyrotech. **33**, 122 (2008).
[15]E. M. Hunt, S. Malcolm, M. L. Pantoya, and F. Davis, Int. J. Impact. Eng. **36**, 842 (2009).
[16]V. Sanders, B. Asay, T. Foley, B. Tappan, A. Pacheco, S. Son, J. Propul. Power. **23**, 707 (2007).
[17]K. S. Martirosyan, L. Wang, A. Vicent, and D. Luss, Nanotechnology **20**, 405609 (2009).
[18]K. S. Martirosyan and D. Luss, Chem. Eng. Technology. **32**, 1376 (2009).
[19]M. J. Starink, Thermochim. Acta. **404**, 163 (2003).
[20]L. P. H. Jeurgens, W. G. Sloof, F. D. Tichelaar, and E. J. Mittemeijer, J. Appl. Phys. **92**, 1649 (2002).
[21]F. Shimojo, A. Nakano, R. K. Kalia, and P. Vashishta, Appl. Phys. Lett. **95**, 043114 (2009).
[22]R. J. Jouet, A. D. Warren, D. M. Rosenberg, V. J. Bellitto, K. Park, and M. R. Zachariah, Chem. Mater. **17**, 2987 (2005).
[23]B. Dikici, S. W. Dean, M. L. Pantoya, V. I. Levitas, and R. J. Jouet, Energ. Fuel. **23**, 4231 (2009).
[24]F. Shimojo, A. Nakano, R. K. Kalia, and P. Vashishta, Phys. Rev. E. **77**, 066103 (2008).
[25]K. W. Watson, M. L. Pantoya, V. I. Levitas, Combust. Flame. **155**, 619 (2008).
[26]V. I. Levitas, B. W. Asay, S. F. Son, and M. Pantoya, J. Appl. Phys. **101**, 083524 (2007).
[27]A. Rai, K. Park, L. Zhou, and M. R. Zachariah, Combust. Theor. Model. **10**, 843 (2006).
[28]S. Chowdhury, K. Sullivan, N. Piekiel, L. Zhou, and M. R. Zachariah, J. Phys. Chem. C. **114**, 9191 (2010).
[29]A. Rai, D. Lee, K. Park, and M. R. Zachariah, J. Phys. Chem. B. **108**, 14793 (2004).
[30]A. Ermoline and E. L. Dreizin, Chem. Phys. Lett. **505**, 47 (2011).
[31]V. P. Zhdanov and B. Kasemo, Chem. Phys. Lett. **452**, 285 (2008).
[32]B. J. Henz, T. Hawa, and M. R. Zachariah, J. Appl. Phys. **107**, 024901 (2010).
[33]R. Nakamura, D. Tokozakura, H. Nakajima, J. G. Lee, and H. Mori, J. Appl. Phys. **101**, 074303 (2007).
[34]G. Chauhan, M. S. Thesis, Texas Tech University, Lubbock, TX, 2007.
[35]C. A. Johnson, Surf. Sci. **3**, 429 (1965).
[36]Q. Jiang, C. C. Yang, and J. C. Li, Mater. Lett. **56**, 1019 (2002).
[37]M. A. Trunov, M. Schoenitz, and E. L. Dreizin, Combust. Theor. Model. **10**, 603 (2006).
[38]M. A. Trunov, M. Schoenitz, X. Zhu, and E. L. Dreizin, Combust. Flame. **140**, 310 (2005).
[39]R. Friedman and A. Macek, Combust. Flame. **6**, 9 (1962).
[40]A. G. Merzhanov, Y. M. Grigorjev, and Y. A. Gal'chenko, Combust. Flame. **29**, 1 (1977).